



RESEARCH ARTICLE

Open Access

Archaeological and archaeometric study of the glass finds from the ancient harbour of Classe (Ravenna- Italy): new evidence

Sarah Maltoni^{1*}, Tania Chinni², Mariangela Vandini³, Enrico Cirelli², Alberta Silvestri⁴ and Gianmario Molin¹

Abstract

Introduction: The present study focuses on Late-Roman/Early Medieval glass found in the productive area within the ancient harbour of Classe near Ravenna, one of the most important trade centres between the 5th and 8th centuries AD of the Northern Adriatic area. Aims of the study were the identification of the main glass compositions and their contextualisation in Late-Antique groups; the identification of provenance of raw glass, and, consequently, of commercial routes; the extent, if any, of recycling glass cullet, as an alternative to the import of fresh raw glass; the identification of possible connections between archaeological typology and glass chemical composition.

Results: 32 glassworking wastes and 25 drinking vessel fragments for a total amount of 57 fragments were devoted to chemical analysis in XRF and EPMA. All the analysed fragments are silica-soda lime glasses, produced with natron as a flux, and are compositionally similar to Late-Antique groups HIMT, Série 3.2 and Levantine1. Raw glass chunks, glassworking wastes and objects of comparable compositions are identified into HIMT and Série 3.2 groups, while the Levantine 1 group includes only objects and glassworking wastes. Systematic comparisons between Classe and Aquileia, the two most important Late-Antique archaeological sites of North-Eastern Italy, were also carried out, and the same compositional groups were identified, although Série 3.2 in the Classe assemblage is more represented. Sr and Nd isotopic analysis confirmed that the composition of the three glasses derive from coastal sands of the Syro-Palestinian and Egyptian shore, with a slight shift in comparison to the published data. Little evidence of recycling was identified in the assemblage.

Conclusions: In the 5th century, a secondary glass workshop devoted to the shaping of glass vessels starting from raw glass chunks and, possibly, glass cullet, was active in the area of the harbour. Raw glass of HIMT and Série 3.2 was imported from the Levant and Egypt. Comparisons between Classe and Aquileia show that during the Late Antiquity these sites seem to be supplied of raw glass by the same trade routes. In addition, some connections between types and chemical compositions were highlighted.

Keywords: Glass, Late-Antiquity, Classe, Chemical composition, Production technology, Provenance, Strontium, Neodymium, Isotopes

Introduction

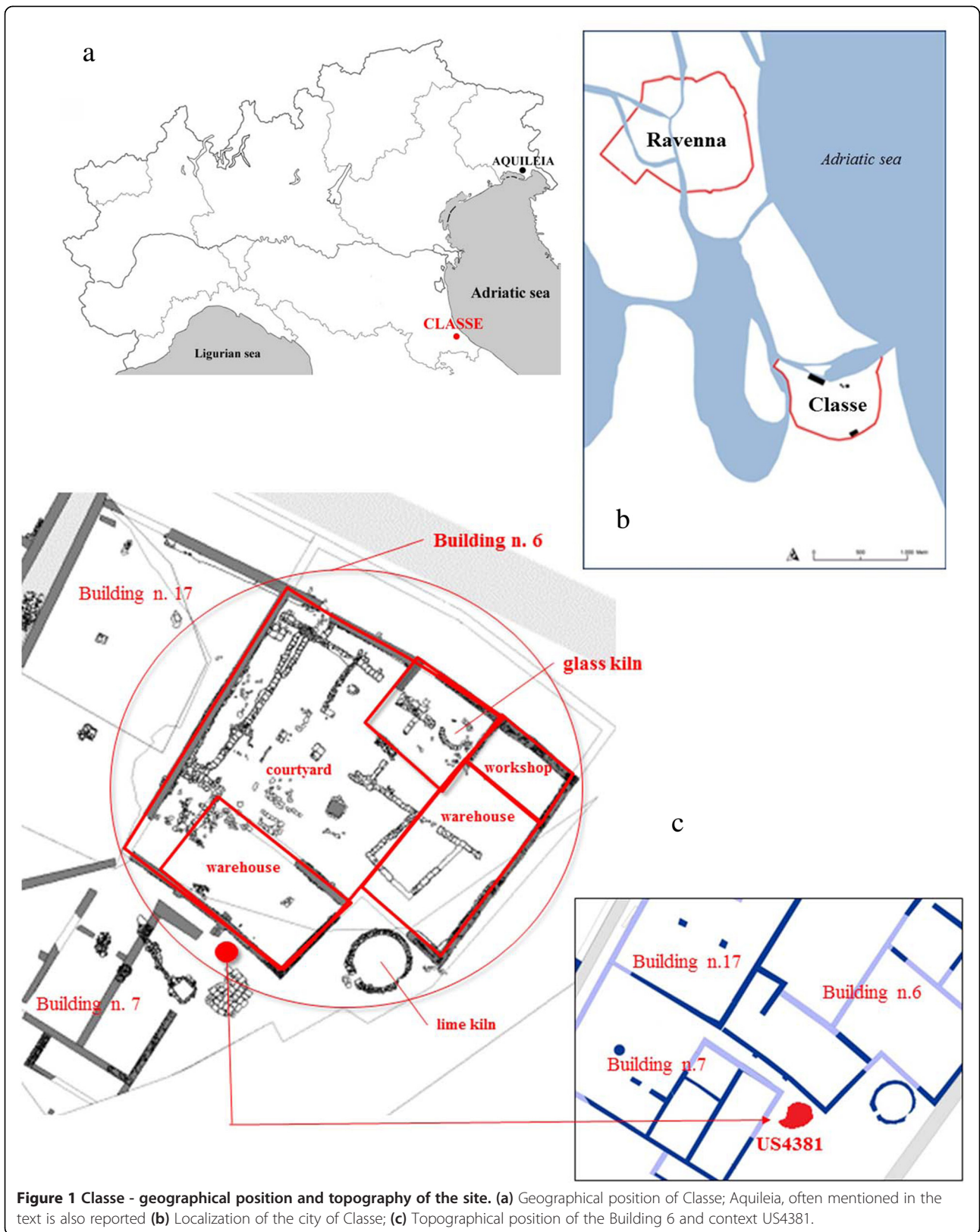
The present study is part of a wider research project about glass production, trade and consumption in the North Adriatic Italy, covering the time interval between the Early Iron Age and the Middle Ages. In particular, this paper focuses on Late-Roman/Early Medieval glass found in the area of the ancient harbour of Classe near

Ravenna, one of the most important trade centres between the 5th and 8th centuries AD of the Northern Adriatic area [Figure 1a]. This area is particularly interesting not only because it is located between Eastern Mediterranean and continental Europe but also because, especially during the Late Antiquity, the relevance of Adriatic trade routes connecting continental Europe with the Levant increases, due to the great political changes that followed the fall of the Roman Empire and the consequent increasing key role played by the Eastern Mediterranean area.

* Correspondence: sarah.maltoni@gmail.com

¹Dipartimento di Beni Culturali, Università degli Studi di Padova, piazza Capitaniato 3, Padova, Italy

Full list of author information is available at the end of the article



In this context, in the 5th century AD the city of Ravenna became the Imperial See of the Western Roman Empire. The imperial court required a large quantity of goods and a great system of infrastructure was realized to support the increasing maritime traffic from the Levant to the city of Ravenna [Figure 1b]. During the recent excavations of the harbour area of Classe, a large amount of glass was recovered and evidence of glass working was identified [1,2]. Although the archaeological study of the glass allows us to exclude primary production in the area under investigation and seems to support the centralised production model, in which raw glass is produced in a few primary production location and then exported to secondary workshops for vessel shaping [3-5], the present study, combining archaeological and archaeometric data, aims to answer various questions still open. These are mainly related to: 1) identification of the main glass compositions worked in Classe and their contextualisation in Late-Antique groups, reported in the literature until now; 2) identification of provenance of raw glass worked in Classe, and, consequently, of the glass commercial routes; 3) extent, if any, of practice of recycling glass cullet, as an alternative to the import of fresh raw glass; 4) identification of eventual correlations between archaeological types and glass chemical composition.

Archaeological context

Classe was located on the Adriatic Sea and connected to the city of Ravenna by a canal system. The topography of the port area suggests that it was planned since its origins with streets, a drainage system and at least eighteen buildings, probably warehouses, mainly devoted to the storage of foodstuff coming from East Mediterranean and Carthage [6]. In some cases the excavations of the warehouses brought to light also raw materials, such as iron slabs and, in one case, slags and traces of iron forging were found close to one of the warehouses dated to the 5th century. The productive vocation of the port area is also confirmed by the glassworking evidence excavated in Classe between 2001 and 2005. The main context for glassworking was identified inside one of the warehouses, named Building 6, built at the beginning of the 5th century. The building is divided in four different rooms, in one of which a small circular kiln was identified [Figure 1c]. Around the small circular kiln a massive concentration of glass fragments and glassworking wastes was found in the excavation of 2001 [2]. So far, the most likely hypothesis is that the small kiln, discovered in the 1970s and initially ascribed to ceramic production, can now be recognized as a glass-furnace.

The archaeological data allow us to state that the main glassworking activity took place in Classe in the 5th century.

Another interesting glass assemblage was excavated in a further context of the port area, here named US4381, and constituted by a small dump dated between the end of the 5th and the beginning of the 6th century AD. This dump is also particularly relevant because of its location, close to the remarkable warehouse named Building 17 [7,8]. The importance of the Building 17, abandoned after a fire at the end of the 5th century, is related to its content, constituted by Tunisian amphorae, lamps and fine wares. In the small context US4381 a second group of vessels and wastes was excavated. Differing from Building 6, where the glass assemblage is related to productive activity in Classe, the excavation of the dump US4381 can give interesting information about glass consumption in the area under investigation. The cross-analysis of both contexts may provide a complete view of the glass life-cycle in Classe.

The glass assemblage

Among the warehouses of the harbour of Classe, Building 6 stands out for the number and variety of glass finds retrieved: 973 working indicators (raw glass chunks and scraps) and 540 fragments of vessels, 257 of which recognised as specific forms: beakers (33%), goblets (15%), bottles/jars (10%), bowls (10%) and lamps (5%) for a total amount of 1513 glass fragments. All the identifiable materials are dated to the 5th - 8th century AD; more represented are those forms dated between the 5th and 6th centuries, coinciding with the period of greatest use of the warehouse.

Among the discoveries of Building 6, beakers are the most attested form, particularly types Isings 96, Isings 106 (with the two variants 106b - with rounded rim - and 106c - with unfinished rim), Isings 107 and Isings 109 were identified. Among the drinking vessels, a high percentage of goblets Isings 111 are recorded, a common situation found within the most important sites of the Mediterranean area in the Late Antiquity [9-15].

From the US4381 excavation, a small number of glassworking indicators (16) and some fragments of glass vessels (213) were recovered. Among the vessels, well represented are the drinking vessels (34%) in particular beakers (32%), followed by bowls (24%), lamps (22%), and bottles/jars (14%). The dating of all the identified forms is confirmed by stratigraphic data.

In both the archaeological context under investigation, beakers and goblets are the most common types found. A selection of beakers and goblets from the two contexts was devoted to archaeometric analysis. In order to gain information about the activity of the glass *atelier*, a selection of working indicators was also here analysed. The full archaeological data of the selected assemblage is summarised in [Tables 1 and 2].

The quality of the glass is generally low in all the analysed vessels: air bubbles, blowing traces and mainly

Table 1 List of analysed vessel glass fragments from Classe

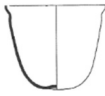
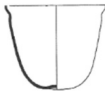
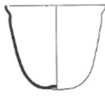
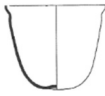

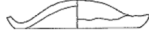







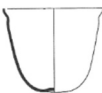


Sample	Macro-type	Type	Drawing	Form dating	Colour
BUILDING 6					
D1	Beaker	ls. 96		4 th – 5 th	Green
D2	Beaker	ls. 96		4 th – 5 th	Green
D3	Beaker	ls. 96		4 th – 5 th	Green
D5	Beaker	ls. 96		4 th – 5 th	Green
D7	Beaker	ls. 109		4 th – 5 th	Blue
D8	Beaker	ls. 96/106c/109		4 th – 5 th	Green
D10	Goblet	ls. 111		5 th – 8 th	Light Blue
D11	Goblet	ls. 111		5 th – 8 th	Colourless
D14	Goblet	ls. 111		5 th – 8 th	Colourless
D16	Beaker	ls.109	see D7	4 th – 5 th	Colourless
D20	Beaker	ls. 106b		5 th – 6 th	Green
D21	Beaker	ls. 106b		5 th – 6 th	Green
D23	Beaker	ls. 109	see D7 and D16	4 th – 5 th	Light Blue
D24	Beaker	ls. 109		4 th – 5 th	Green
D25	Beaker	ls. 96/106c/109	see D8	4 th – 5 th	Light Blue
D26	Beaker	ls. 107		4 th – 5 th	Blue
US4381					
D50	Beaker	ls. 106b		5 th – 6 th	Brown
D51	Beaker	ls. 106c		5 th – 6 th	Colourless
D52	Beaker	Sternini 1995, p. 275, Figure seven, tav. 60 (ls. 106 late)		5 th – 6 th	Green

Table 1 List of analysed vessel glass fragments from Classe (Continued)

D53	Goblet?	Is. 111?		5 th – 8 th	Green
D54	Beaker	Is. 96		4 th – 5 th	Green
D56	Beaker	Is. 96c	see D54	4 th – 5 th	Green
D57	Beaker	Sternini 1995, p. 276, Figure eight, tav. 77 (Is. 106 late)		5 th – 6 th	Colourless
D58	Beaker	Sternini 1995, p. 276, Figure eight, tav. 68. (Is. 106 late)		5 th – 6 th	Colourless
D59	Beaker	Is. 106 late	see D50	5 th – 6 th	Colourless

Forms are classified after Isings, [16]; when not applicable, references to other typological classifications are given [17].

unintentional colour (generally with various shade of green) seem to support the hypothesis of a not very refined productions.

Both the contexts show a high degree of fragmentation of the artefacts; in the case of Building 6, this can be due to cullet collection for recycling purpose; in the case of the US4381, the high fragmentation of this part of assemblage is consistent with the function of the context, that is meant to host waste.

Experimental

32 glassworking wastes and 25 vessel fragments for a total amount of 57 fragments were selected for the archaeometric analyses from the whole glass assemblage found in the areas named Building 6 and US4381 of Classe. To characterise the samples the following complementary techniques were used: Optical Microscopy (OM) for preliminary morphological observations, X-Ray Fluorescence (XRF) and Electron Probe Micro Analysis (EPMA) for chemical bulk composition, Multi Collector-Inductively Coupled Plasma-Mass Spectrometry (MC-ICP-MS) for the determination of Sr and Nd isotopic ratios.

Some of the samples were previously analysed and published [18,19] and were here reconsidered for the comparative purposes of this work. In order to guarantee the full comparability among the samples and to reduce the influence of a systematic error, chemical analyses were newly performed under the same analytical conditions on all the fragments.

Sampling

In order to avoid contamination, all the fragments were carefully cleaned and the outer layers were removed by a diamond drill.

For EPMA analysis, small fragment of each sample were cut perpendicularly to the surface with a diamond-coated saw and embedded in epoxy resin blocks. The surface of each sample was then polished with a series of diamond pastes down to 1 μm grade and coated with conductive carbon film.

For the samples devoted to XRF analysis, 700 mg of each sample were grounded into powder in an agate mortar and put in an oven at 110°C for 12 hours. The powders were then mixed with $\text{Li}_2\text{B}_4\text{O}_7$ in a 1:10 ratio and beads were prepared.

For the isotopic analysis, further 100 mg from selected samples were reduced in powder in an agate mortar.

Techniques and analytical conditions

OM observations were carried out under stereoscopic vision on the whole fragment with a Zeiss Stemi 2000C microscope and, under reflected light, on polished sections with a Nikon Eclipse ME600, both supplied by the Department of Geosciences, University of Padova (Italy). These observations revealed the substantial homogeneity of all samples under investigation, including all the glassworking wastes.

The bulk chemical composition of 31 samples was measured by XRF, using a Philips PW 2400 instrument, equipped with a Rh tube with a power supply of 3 kW (60 kV/125 mA max.). This technique allowed to determine all the elements listed in [Tables 3 and 4], with the exception of S, Cl, Sn, Sb that were measured by EPMA.

The bulk chemical composition of the smaller samples was determined by EPMA on polished sections. The electron probe used for quantitative micro-analysis is a Cameca SX50, equipped with four wavelength-dispersive spectrometers. An average of 6 random analytical points was performed on each sample, and mean

Table 2 List of analysed glassworking indicators fragments from Classe








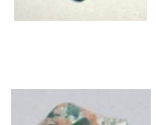



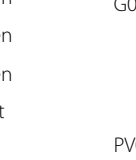

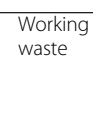
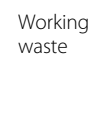
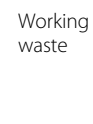

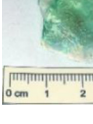


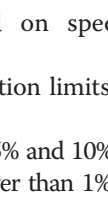
Sample	Macro-type	Type	Photo	Colour
BUILDING 6				
A2	Working waste	Waste		Green
A3	Working waste			Green
BL SCH	Working waste	Waste		Green
BLC				Light Blue
BLS				Green
C4	Working waste	Tubes		Green
CVC				Green
CVG				Green/Yellow
CVS				Green
TB				Green
FD	Working waste	Deformed fragment		Green
FD D12	Working waste	Deformed fragment		Light Blue
G1	Working waste	Pontil wad		Green
G3	Working waste	Pontil wad		Yellow
G4	Working waste	Pontil wad		Green
GRA	Working waste	Pontil wad		Light Blue
M1	Working waste	Moil		Green/Yellow
PF	Working waste	Drop		Green
PV	Working waste	Raw Chunk		Green
PVA	Working waste	Raw Chunk		Green
PVC	Working waste	Raw Chunk		Light Blue
PVM	Working waste	Raw Chunk		Green/Brown

Table 2 List of analysed glassworking indicators fragments from Classe (Continued)

	Working waste			
PVS	Working waste			Green
SCH	Working waste	Bubbly waste		Green
T-A	Working waste	Shearing		Green
T-C	Working waste	Shearing		Green/Yellow
US4381				
G05	Working waste	Pontil wad		Green
G06	Working waste	Pontil wad		Light Blue
PV01	Working waste	Raw Chunk		Green
T04	Working waste	Shearing		Light Blue
T10	Working waste	Shearing		Green
T12	Working waste	Shearing		Colourless

and standard deviation were calculated on specific compositional groups.

Details of analytical conditions and detection limits for EPMA are reported in [20].

Precision of EPMA analysis was between 0.5% and 10% for major and minor elements. Accuracy was lower than 1% for Si, Na, and Fe, lower than 5% for minor elements, and not higher than 12% for trace elements. XRF precision was better than 0.6% for major and minor elements, and about 3% for trace elements; accuracy was within 0.5% for Si, lower than 3% for other major and minor elements, and lower than 5% for traces. Detailed information about precision and accuracy are reported in [21].

The results of both XRF and EPMA chemical analysis are listed in Tables 3 and 4. Major elements are expressed in weight percent of the corresponding oxide, while the trace elements are reported in parts per million (ppm). In the case

Table 3 Chemical composition of the samples - Major and minor elements

Group	Sample	Context	Macro-type	Type	Technique	SiO ₂	Na ₂ O	CaO	Al ₂ O ₃	Fe ₂ O ₃	MnO	TiO ₂	MgO	K ₂ O	P ₂ O ₅	SO ₃	Cl
CL1a	D1	Building 6	beaker	ls. 96	EPMA	63.71	18.45	6.22	3.07	3.17	1.87	0.60	1.53	0.54	0.10	0.26	1.07
CL1a	D3	Building 6	beaker	ls. 96	EPMA	65.63	18.66	5.86	2.42	3.12	2.12	0.31	0.97	0.43	0.06	0.06	1.30
CL1a	D5	Building 6	beaker	ls. 96	XRF+ EPMA	64.30	17.76	5.59	2.97	3.52	1.85	0.62	1.20	0.45	0.14	0.25	1.20
CL1a	A2	Building 6	waste	waste	XRF+ EPMA	64.73	17.71	6.11	3.1	3.4	1.17	0.54	1.37	0.53	0.13	0.21	1.30
CL1a	BLS	Building 6	waste	waste	XRF+ EPMA	64.56	16.54	6.05	3.08	3.84	2.08	0.62	1.35	0.50	0.16	0.25	1.09
CL1a	CVG	Building 6	waste	tubes	XRF+ EPMA	64.09	16.45	6.15	2.98	4.12	1.83	0.54	1.36	1.08	0.13	0.19	1.26
CL1a	PVM	Building 6	waste	raw chunck	XRF+ EPMA	64.83	16.82	6.03	2.94	3.6	1.66	0.55	1.35	0.39	0.13	0.19	1.25
CL1a	PVS	Building 6	waste	raw chunck	XRF+ EPMA	64.12	18.34	5.99	3.04	3.19	1.57	0.54	1.54	0.40	0.11	0.29	1.58
CL1a	TB	Building 6	waste	tubes	XRF+ EPMA	64.89	16.80	6.18	3.02	3.56	1.64	0.54	1.36	0.95	0.12	0.17	1.41
CL1b	D2	Building 6	beaker	ls. 96	EPMA	66.18	17.77	6.79	2.84	2.46	1.73	0.44	1.36	0.55	0.05	0.25	0.89
CL1b	D8	Building 6	beaker	ls. 96/106/109	XRF+ EPMA	64.56	16.87	7.33	2.86	2.89	1.50	0.45	1.21	0.64	0.16	0.26	0.89
CL1b	D20	Building 6	beaker	ls. 106b	EPMA	65.66	17.77	6.08	2.82	2.27	1.54	0.48	1.24	0.54	0.04	0.22	1.02
CL1b	D24	Building 6	beaker	ls. 109	XRF+ EPMA	63.08	21.17	5.15	2.80	1.83	2.51	0.60	0.93	0.34	0.04	0.16	1.44
CL1b	D26	Building 6	beaker	ls. 107	EPMA	66.47	18.11	5.79	2.97	1.84	0.13	0.43	1.10	0.40	0.01	0.27	1.48
CL1b	BL SCH	Building 6	waste	waste	EPMA	63.94	18.07	6.16	3.01	2.68	1.86	0.45	1.77	0.85	0.13	0.19	1.38
CL1b	CVS	Building 6	waste	tubes	XRF+ EPMA	66.04	17.67	4.78	3.07	2.09	2.44	0.69	1.48	0.63	0.05	0.19	1.29
CL1b	FD	Building 6	waste	deformed fragment	XRF+ EPMA	67.53	16.08	6.22	3.03	2.40	1.22	0.60	1.47	0.48	0.06	0.13	1.40
CL1b	PF	Building 6	waste	drop	EPMA	62.31	18.97	5.86	2.94	2.24	2.32	0.62	1.82	1.09	0.11	0.51	1.49
CL1b	SCH	Building 6	waste	bubbly waste	EPMA	63.44	18.70	5.87	2.86	2.11	2.54	0.58	2.13	0.85	0.09	0.25	1.23
CL1b	D52	US4381	beaker	ls. 106 late	EPMA	65.47	16.97	8.17	2.62	1.51	2.06	0.19	1.53	0.73	0.21	0.25	0.95
CL1b	D53	US4381	goblet	ls. 111?	EPMA	64.77	18.67	5.50	3.08	1.98	2.55	0.58	1.49	0.44	0.01	0.20	1.27
CL1b	D54	US4381	beaker	ls. 96	EPMA	68.63	17.24	5.81	2.42	1.38	2.28	0.25	0.87	0.38	0.03	0.21	1.10
CL1b	D56	US4381	beaker	ls. 96	EPMA	67.95	17.90	6.01	2.38	1.50	2.25	0.26	0.94	0.40	0.06	0.20	1.25
CL1b	PV01	US4381	waste	raw chunck	EPMA	65.13	20.64	5.92	2.25	1.37	1.98	0.30	1.31	0.32	0.04	0.20	1.67
CL1c	D50	US4381	beaker	ls. 106b	EPMA	65.34	19.35	7.69	2.23	0.81	1.78	0.14	1.00	0.53	0.12	0.33	1.13
CL1c	T12	US4381	waste	shearing	EPMA	65.44	18.47	7.59	2.55	1.05	1.13	0.14	1.31	0.66	0.11	0.22	1.14
CL2a	D21	Building 6	beaker	ls. 106	EPMA	68.01	16.52	9.92	2.81	0.30	0.03	0.07	0.67	0.86	0.03	0.14	1.08
CL2b	C4	Building 6	waste	tubes	XRF + EPMA	68.21	14.87	9.63	2.94	0.64	0.66	0.09	0.65	1.40	0.20	0.09	1.06
CL2b	D58	US4381	beaker	ls. 106 late	EPMA	68.02	16.39	8.19	2.86	0.33	0.90	0.05	0.54	1.00	0.16	0.18	1.06
CL2a	G05	US4381	waste	pontil wad	EPMA	69.25	15.21	7.91	2.81	0.46	0.03	0.09	0.61	2.46	0.15	0.11	1.17
CL2a	T04	US4381	waste	shearing	EPMA	70.34	16.01	7.87	2.86	0.43	0.03	0.08	0.62	0.82	0.08	0.15	1.03
CL2b	T10	US4381	waste	shearing	EPMA	65.91	15.21	10.57	2.91	0.62	0.89	0.10	0.64	2.03	0.31	0.15	0.50
CL3	D7	Building 6	beaker	ls. 109	EPMA	68.76	19.02	5.70	1.96	2.14	0.34	0.12	0.51	0.55	0.02	0.27	0.90

Table 3 Chemical composition of the samples - Major and minor elements (Continued)

CL3	D10	Building 6	goblet	ls. 111	EPMA	68.07	21.10	6.26	1.97	0.65	0.82	0.13	0.77	0.40	0.01	0.29	1.26
CL3	D11	Building 6	goblet	ls. 111	EPMA	68.29	18.17	6.93	2.04	0.98	0.77	0.12	0.71	0.43	0.01	0.22	1.07
CL3	D14	Building 6	goblet	ls. 111	EPMA	69.05	20.02	6.99	1.56	0.38	0.72	0.09	0.62	0.37	0.00	0.31	1.29
CL3	D16	Building 6	beaker	ls. 109	XRF+ EPMA	69.91	19.06	6.16	1.58	0.30	0.50	0.06	0.30	0.41	0.04	0.17	1.73
CL3	D23	Building 6	beaker	ls. 109	XRF+ EPMA	71.96	17.39	4.95	1.94	0.61	0.74	0.18	0.49	0.47	0.03	0.12	1.52
CL3	D25	Building 6	beaker	ls. 96/106/109	XRF+ EPMA	71.09	17.89	5.55	1.76	0.45	0.75	0.08	0.48	0.36	0.03	0.11	1.59
CL3	A3	Building 6	waste	waste	XRF+ EPMA	68.15	19.41	6.28	1.84	0.78	0.58	0.12	0.59	0.57	0.04	0.27	1.45
CL3	BLC	Building 6	waste	waste	XRF+ EPMA	67.06	17.42	8.14	2.23	0.96	0.29	0.18	0.94	0.86	0.06	0.35	1.03
CL3	CVC	Building 6	waste	tubes	XRF+ EPMA	68.3	18.97	6.14	1.83	0.82	0.61	0.12	0.61	0.72	0.05	0.33	1.24
CL3	F-D D12	Building 6	waste	deformed fragment	XRF+ EPMA	67.12	19.74	7.59	1.85	0.67	0.59	0.11	0.60	0.48	0.04	0.17	1.70
CL3	G1	Building 6	waste	pontil wad	EPMA	66.78	18.57	8.17	1.94	0.65	0.36	0.13	0.84	0.63	0.01	0.36	1.13
CL3	G3	Building 6	waste	pontil wad	EPMA	68.08	17.85	6.92	2.38	0.26	0.76	0.07	0.40	1.50	0.01	0.36	1.22
CL3	G4	Building 6	waste	pontil wad	EPMA	67.11	17.63	6.50	2.38	1.25	1.35	0.27	1.00	0.88	0.01	0.36	1.14
CL3	GRA	Building 6	waste	pontil wad	XRF+ EPMA	68.97	19.31	5.89	1.75	0.56	0.83	0.09	0.58	0.84	0.03	0.29	1.32
CL3	M1	Building 6	waste	moil	EPMA	69.18	18.66	6.80	2.12	0.77	0.98	0.21	0.73	0.42	0.04	0.21	1.28
CL3	PV	Building 6	waste	raw chunk	XRF+ EPMA	66.51	19.80	5.87	2.12	1.41	0.85	0.23	0.81	0.43	0.06	0.24	1.38
CL3	PVA	Building 6	waste	raw chunk	XRF+ EPMA	66.92	17.98	8.16	2.15	0.88	0.29	0.17	0.89	0.65	0.05	0.32	1.34
CL3	PVC	Building 6	waste	raw chunk	XRF+ EPMA	69.04	19.38	6.11	1.77	0.65	0.51	0.1	0.56	0.44	0.04	0.35	1.23
CL3	T-A	Building 6	waste	shearing	XRF+ EPMA	66.52	19.34	8.01	1.99	0.71	0.13	0.15	0.81	0.62	0.04	0.31	1.38
CL3	T-C	Building 6	waste	shearing	EPMA	67.82	19.76	6.50	1.78	0.58	0.52	0.11	0.64	0.44	0.02	0.32	1.19
CL3	D51	US4381	beaker	ls. 106c	EPMA	67.93	18.16	7.90	1.94	0.86	0.77	0.12	0.71	0.55	0.09	0.24	1.30
CL3	D57	US4381	beaker	ls. 106late	EPMA	69.06	18.08	6.79	1.77	0.61	0.62	0.11	0.58	0.47	0.08	0.27	1.25
CL3	D59	US4381	beaker	ls. 106 late	EPMA	67.86	19.18	7.45	1.73	0.61	0.74	0.10	0.65	0.35	0.08	0.29	1.22
CL3	G06	US4381	waste	waste	EPMA	66.60	21.85	5.75	1.80	0.52	0.96	0.11	0.62	0.30	0.02	0.44	1.23

Major and minor elements are reported in wt%. EPMA indicates that chemical data were collected with this technique only; EPMA+ XRF indicates samples were analysed by XRF for their major, minor and trace elements while Sn, Sb, Cl and S were measured with EPMA. SnO₂ and Sb₂O₃ were always below the EPMA detection limits (0.04 wt%) and are not presented here. n.d. = not detected.

Table 4 Chemical composition of the samples - Trace elements

Group	Sample	Context	Macro-type	Type	Technique	Co	Cu	Pb	V	Cr	Ni	Zn	Rb	Sr	Y	Zr	Nb	Ba	La	Ce	Nd
CL1a	D1	Building 6	beaker	ls. 96	EPMA	<200	900	6500	n.d.	n.d.	n.d.	<321	n.d.	n.d.	n.d.	n.d.	n.d.	n.d.	n.d.	n.d.	n.d.
CL1a	D3	Building 6	beaker	ls. 96	EPMA	<200	<265	<696	n.d.	n.d.	n.d.	<321	n.d.	n.d.	n.d.	n.d.	n.d.	n.d.	n.d.	n.d.	n.d.
CL1a	D5	Building 6	beaker	ls. 96	XRF + EPMA	7	98	35	99	83	44	67	11	413	16	289	4	257	11	18	30
CL1a	A2	Building 6	waste	waste	XRF + EPMA	9	79	31	110	74	36	42	14	419	15	226	5	266	34	15	36
CL1a	BLS	Building 6	waste	waste	XRF + EPMA	18	133	125	107	83	54	55	14	474	18	273	6	299	17	10	26
CL1a	CVG	Building 6	waste	tubes	XRF + EPMA	17	125	145	128	73	44	54	29	493	20	231	8	378	<10	<10	14
CL1a	PVM	Building 6	waste	raw chunk	XRF + EPMA	17	104	57	118	76	68	48	12	457	15	212	6	376	<10	15	16
CL1a	PVS	Building 6	waste	raw chunk	XRF + EPMA	11	96	169	84	70	34	81	10	451	17	240	8	288	25	21	26
CL1a	TB	Building 6	waste	tubes	XRF + EPMA	15	119	48	118	68	34	50	28	505	15	236	7	380	<10	14	18
CL1b	D2	Building 6	beaker	ls. 96	EPMA	<200	<265	<696	n.d.	n.d.	n.d.	<321	n.d.	n.d.	n.d.	n.d.	n.d.	n.d.	n.d.	n.d.	n.d.
CL1b	D8	Building 6	beaker	ls. 96/106/109?	XRF + EPMA	22	119	181	87	61	31	51	12	601	17	201	25	374	<10	13	21
CL1b	D20	Building 6	beaker	ls. 106	EPMA	<200	<265	<696	n.d.	n.d.	n.d.	<321	n.d.	n.d.	n.d.	n.d.	n.d.	n.d.	n.d.	n.d.	n.d.
CL1b	D24	Building 6	beaker	ls. 109	XRF + EPMA	12	65	17	66	79	65	30	10	380	12	261	5	1181	<10	27	<10
CL1b	D26	Building 6	beaker	ls. 107	EPMA	1212	1795	1377	n.d.	n.d.	n.d.	<321	n.d.	n.d.	n.d.	n.d.	n.d.	n.d.	n.d.	n.d.	n.d.
CL1b	BL SCH	Building 6	waste	waste	EPMA	<200	<265	<696	n.d.	n.d.	n.d.	<321	n.d.	n.d.	n.d.	n.d.	n.d.	n.d.	n.d.	n.d.	n.d.
CL1b	CVS	Building 6	waste	tubes	XRF + EPMA	20	43	111	107	91	34	42	15	527	16	295	7	739	<10	22	<10
CL1b	FD	Building 6	waste	deformed fragment	XRF + EPMA	11	54	24	82	73	21	34	12	443	14	268	30	267	<10	26	25
CL1b	PF	Building 6	waste	drop	EPMA	<200	<265	<696	n.d.	n.d.	n.d.	<321	n.d.	n.d.	n.d.	n.d.	n.d.	n.d.	n.d.	n.d.	n.d.
CL1b	SCH	Building 6	waste	bubbly waste	EPMA	<200	<265	<696	n.d.	n.d.	n.d.	<321	n.d.	n.d.	n.d.	n.d.	n.d.	n.d.	n.d.	n.d.	n.d.
CL1b	D52	US4381	beaker	ls. 106 late	EPMA	<200	0.02	<696	n.d.	n.d.	n.d.	<321	n.d.	n.d.	n.d.	n.d.	n.d.	n.d.	n.d.	n.d.	n.d.
CL1b	D53	US4381	goblet?	ls. 111?	EPMA	<200	<265	<696	n.d.	n.d.	n.d.	<321	n.d.	n.d.	n.d.	n.d.	n.d.	n.d.	n.d.	n.d.	n.d.
CL1b	D54	US4381	beaker	ls. 96	EPMA	<200	<265	<696	n.d.	n.d.	n.d.	<321	n.d.	n.d.	n.d.	n.d.	n.d.	n.d.	n.d.	n.d.	n.d.
CL1b	D56	US4381	beaker	ls. 96	EPMA	<200	<265	<696	n.d.	n.d.	n.d.	<321	n.d.	n.d.	n.d.	n.d.	n.d.	n.d.	n.d.	n.d.	n.d.
CL1b	PV01	US4381	waste	raw glass chunk	EPMA	<200	<265	<696	n.d.	n.d.	n.d.	<321	n.d.	n.d.	n.d.	n.d.	n.d.	n.d.	n.d.	n.d.	n.d.
CL1c	D50	US4381	beaker	ls. 106	EPMA	<200	<265	<696	n.d.	n.d.	n.d.	<321	n.d.	n.d.	n.d.	n.d.	n.d.	n.d.	n.d.	n.d.	n.d.
CL1c	T12	US4381	waste	shearing	EPMA	<200	<265	<696	n.d.	n.d.	n.d.	<321	n.d.	n.d.	n.d.	n.d.	n.d.	n.d.	n.d.	n.d.	n.d.
CL2a	D21	Building 6	beaker	ls. 106	EPMA	<200	<265	<696	n.d.	n.d.	n.d.	<321	n.d.	n.d.	n.d.	n.d.	n.d.	n.d.	n.d.	n.d.	n.d.
CL2b	C4	Building 6	waste	tubes	XRF + EPMA	5	44	119	21	17	8	77	20	504	10	49	3	327	<10	11	23
CL2b	D58	US4381	beaker	ls. 106 late	EPMA	<200	<265	<696	n.d.	n.d.	n.d.	<321	n.d.	n.d.	n.d.	n.d.	n.d.	n.d.	n.d.	n.d.	n.d.
CL2a	G05	US4381	waste	pontil wad	EPMA	<200	<265	<696	n.d.	n.d.	n.d.	<321	n.d.	n.d.	n.d.	n.d.	n.d.	n.d.	n.d.	n.d.	n.d.
CL2a	T04	US4381	waste	shearing	EPMA	<200	<265	<696	n.d.	n.d.	n.d.	<321	n.d.	n.d.	n.d.	n.d.	n.d.	n.d.	n.d.	n.d.	n.d.

Table 4 Chemical composition of the samples - Trace elements (Continued)

CL2b	T10	US4381	waste	shearing	EPMA	<200	<265	<696	n.d.	n.d.	n.d.	<321	n.d.	n.d.	n.d.	n.d.	n.d.	n.d.	n.d.	n.d.	n.d.
CL3	D7	Building 6	beaker	ls. 109	EPMA	2060	4110	4180	n.d.	n.d.	n.d.	<321	n.d.	n.d.	n.d.	n.d.	n.d.	n.d.	n.d.	n.d.	n.d.
CL3	D10	Building 6	goblet	ls. 111	EPMA	<200	<265	<696	n.d.	n.d.	n.d.	<321	n.d.	n.d.	n.d.	n.d.	n.d.	n.d.	n.d.	n.d.	n.d.
CL3	D11	Building 6	goblet	ls. 111	EPMA	<200	<265	<696	n.d.	n.d.	n.d.	<321	n.d.	n.d.	n.d.	n.d.	n.d.	n.d.	n.d.	n.d.	n.d.
CL3	D14	Building 6	goblet	ls. 111	EPMA	<200	<265	<696	n.d.	n.d.	n.d.	<321	n.d.	n.d.	n.d.	n.d.	n.d.	n.d.	n.d.	n.d.	n.d.
CL3	D16	Building 6	beaker	ls. 109	XRF + EPMA	3	12	22	16	17	52	14	12	419	5	38	<3	197	<10	<10	11
CL3	D23	Building 6	beaker	ls. 109	XRF + EPMA	7	13	9	35	24	7	15	12	366	7	93	12	226	12	18	21
CL3	D25	Building 6	beaker	ls. 96/106/109	XRF + EPMA	6	11	19	34	14	8	20	11	410	6	43	5	210	26	13	21
CL3	A3	Building 6	waste	waste	XRF + EPMA	3	33	38	24	17	11	21	16	438	8	63	12	208	<10	22	22
CL3	BLC	Building 6	waste	waste	XRF + EPMA	3	23	64	23	26	21	21	17	546	10	92	<3	193	<10	14	23
CL3	CVC	Building 6	waste	tubes	XRF + EPMA	6	38	88	25	24	19	20	23	424	8	64	<3	207	<10	14	20
CL3	F-D D12	Building 6	waste	deformed fragment	XRF + EPMA	4	41	28	32	72	18	22	13	609	8	58	22	205	<10	<10	17
CL3	G1	Building 6	waste	pontil wad	EPMA	<200	<265	<696	n.d.	n.d.	n.d.	<321	n.d.	n.d.	n.d.	n.d.	n.d.	n.d.	n.d.	n.d.	n.d.
CL3	G3	Building 6	waste	pontil wad	EPMA	<200	<265	<696	n.d.	n.d.	n.d.	<321	n.d.	n.d.	n.d.	n.d.	n.d.	n.d.	n.d.	n.d.	n.d.
CL3	G4	Building 6	waste	pontil wad	EPMA	<200	<265	<696	n.d.	n.d.	n.d.	<321	n.d.	n.d.	n.d.	n.d.	n.d.	n.d.	n.d.	n.d.	n.d.
CL3	GRA	Building 6	waste	pontil wad	XRF + EPMA	8	25	34	37	12	8	14	20	430	7	52	<3	222	10	22	14
CL3	M1	Building 6	waste	moil	EPMA EPMA	<200	<265	<696	n.d.	n.d.	n.d.	<321	n.d.	n.d.	n.d.	n.d.	n.d.	n.d.	n.d.	n.d.	n.d.
CL3	PV	Building 6	waste	raw glass chunk	XRF + EPMA	5	53	66	36	31	16	38	12	420	10	107	23	234	<10	23	25
CL3	PVA	Building 6	waste	raw glass chunk	XRF + EPMA	4	19	21	20	83	41	18	13	584	8	88	22	192	<10	26	21
CL3	PVC	Building 6	waste	raw glass chunk	XRF + EPMA	4	29	16	22	16	12	17	12	413	7	55	<3	203	<10	<10	26
CL3	T-A	Building 6	waste	shearing	XRF + EPMA	<3	18	20	16	15	3	17	12	552	9	80	8	169	10	<10	18
CL3	T-C	Building 6	waste	shearing	EPMA	<200	<265	<696	n.d.	n.d.	n.d.	<321	n.d.	n.d.	n.d.	n.d.	n.d.	n.d.	n.d.	n.d.	n.d.
CL3	D51	US 4381	beaker	ls. 106c	EPMA	<200	<265	0.07	n.d.	n.d.	n.d.	<321	n.d.	n.d.	n.d.	n.d.	n.d.	n.d.	n.d.	n.d.	n.d.
CL3	D57	US 4381	beaker	ls. 106late	EPMA	<200	<265	<696	n.d.	n.d.	n.d.	<321	n.d.	n.d.	n.d.	n.d.	n.d.	n.d.	n.d.	n.d.	n.d.
CL3	D59	US 4381	beaker	ls. 106 late	EPMA	<200	<265	<696	n.d.	n.d.	n.d.	<321	n.d.	n.d.	n.d.	n.d.	n.d.	n.d.	n.d.	n.d.	n.d.
CL3	G06	US 4381	waste	waste	EPMA	<200	<265	<696	n.d.	n.d.	n.d.	<321	n.d.	n.d.	n.d.	n.d.	n.d.	n.d.	n.d.	n.d.	n.d.

Trace elements are reported in parts per million (ppm). n.d. = not detected.

of EPMA measurements, mean values are only reported in the tables because the standard deviation is always below 1.65, indicating the substantial homogeneity of the samples.

The chemical data obtained were elaborated with statistical multivariate methods. In order to identify homogeneous compositional groups, hierarchical cluster analysis was conducted with Minitab15 software, using a Ward linkage algorithm and squared Euclidean distance after standardization, taking into account the major elements and excluding the possible intentional colouring and decolouring agents (Sb, Mn). The results obtained are detailed in the “Results and discussion” section.

In order to trace the provenance of the raw materials employed for the primary production of the glass, 12 samples representing the three compositional groups were selected for isotopic analysis.

To separate Sr and Nd from the glass matrix, a chromatographic separation was carried out in a class 10 clean lab at Ghent University (Belgium) following the methods reported in [22] and references therein.

After the separation process, the concentration of both Sr and Nd was checked by a semi-quantitative elemental analysis performed using a Perkin-Elmer SCIEX Elan quadrupole-based ICP-Mass Spectrometer at Ghent University (Belgium). The isotopic ratio for Sr and Nd was then determined by MC-ICP-MS performed with a Thermo-Scientific Neptune instrument at Ghent University (Belgium).

The detailed procedure for Nd isolation, and the full analytical conditions for the elemental analysis and the isotopic ratio determination are reported in [22].

Results and discussion

Chemical analysis

All the analysed samples are silica-soda-lime glasses, with SiO₂ ranging between 62.31 wt% and 71.96 wt%, Na₂O between 14.87 and 21.85 wt%, CaO between 4.78 and 10.60 wt%, Al₂O₃ from 1.54 to 3.08 wt% and Fe₂O₃ from 0.26 to 4.12 wt%. The complete chemical composition of all the samples is given in [Tables 3 and 4]. SnO₂ and Sb₂O₃ were measured by EPMA but, being always below the EPMA detection limits (0.04 wt%), are not reported. The low concentrations of K₂O and MgO, generally below 1.50 wt%, are consistent with the use of natron as flux, according to the Roman and Late-Antique tradition [23].

The multivariate statistical analysis of chemical data allowed us to detect three main groups, here named CL1, CL2 and CL3, whose mean compositions are reported in [Table 5].

Group CL1, that comprises 13 vessel fragments and 13 working indicators, is characterised by high levels of Fe₂O₃ (2.59 ± 0.84 wt%), TiO₂ (0.49 ± 0.14 wt%), Al₂O₃ (2.86 ± 0.25 wt%), MnO (1.86 ± 0.54 wt%) indicating the use of an impure sand as a source of silica, rich in Fe and Ti-bearing minerals. On the basis of the iron content, group CL1 can be subdivided into three subgroups: CL1a composed of 9

samples (3 vessels and 6 glassworking wastes comprehensive of 1 raw chunk), with a very high Fe₂O₃ content (3.38 ± 0.51 wt%), CL1b, composed of 15 samples (9 vessels and 6 glassworking wastes comprehensive of 1 raw chunk), with slightly lower iron (Fe₂O₃ = 2.02 ± 0.48 wt%) and CL1c, composed of two samples both from US4381 (1 vessels and 1 working waste), with lower iron (Fe₂O₃ = 0.93 ± 0.17 wt%). This group shows also lower titanium (TiO₂ = 0.14 wt% in both cases) and alumina (Al₂O₃ = 2.39 ± 0.23 wt%) and higher calcium (CaO = 7.64 ± 0.07 wt%) than CL1a and CL1b.

Group CL2, composed of 4 wastes and 2 vessel fragments, is characterized by high CaO (9.02 ± 1.17 wt%) and alumina (2.86 ± 0.05 wt%) but lower contents of Fe₂O₃, TiO₂ and MnO, indicative of the use of a relative pure siliceous-carbonatic sand. In addition, the relatively elevated content of potash (1.43 ± 0.68 wt%) and alumina of CL2 samples are indicative of the geological origin of the sand, rich in feldspars.

Group CL3, that includes 11 vessel fragment and 14 glassworking wastes comprehensive of 3 raw chunks, can be distinguished from the CL1 and CL2 groups by the low alumina (1.93 ± 0.21 wt%) and lime (6.70 ± 0.92 wt%), suggesting the use of sand less rich in carbonates and feldspars than that employed in CL2 samples [Table 5].

It is interesting to note that both groups CL1 and CL3 include raw chunks, glassworking wastes and objects of comparable compositions while group CL2, which comprises 6 samples only, includes objects and two glassworking wastes but no raw chunk.

The compositional groups identified in Classe were compared with major compositional glass groups dated from the Roman to the Medieval period, as identified in the literature, in order to contextualise the production technologies of this glass assemblage in a wider cultural and geographical framework. In particular, strict and systematic comparisons were also made between glass from Classe and that found in the site of the “*Casa delle Bestie Ferite*” located in Aquileia, the other main important Late-Antique archaeological site of North-Eastern Italy, recently studied by Gallo and co-authors [24] with similar methodological approach. This allows us to better clarify the role of the Northern Adriatic area in the glass production, trade and consumption during the Late-Roman/Early Medieval period.

Comparing the measured data with those reported in the literature for European and Mediterranean glass of comparable dating, it is evident that the composition of all the analysed samples can be put in relation with the Late Antique compositional groups, as clearly shown by the biplot diagram CaO/Al₂O₃ [Figure 2].

In particular, samples belonging to group CL1, due to their high content of iron, manganese, titanium and alumina and soda can be assimilate to those dubbed “HIMT” by Freestone [28] and well documented in the literature (e. g., Group E, [28,29]; Group 2 [25]; HIMT1-2 [30]; Group

Table 5 Mean chemical composition of the groups

Group	SiO ₂	Na ₂ O	CaO	Al ₂ O ₃	Fe ₂ O ₃	MnO	TiO ₂	MgO	K ₂ O	P ₂ O ₅	SO ₃	Cl
CL1a (n = 9)	64.32	17.65	6.00	2.96	3.38	1.81	0.55	1.38	0.63	0.12	0.24	1.30
	<i>0.88</i>	<i>0.94</i>	<i>0.19</i>	<i>0.20</i>	<i>0.51</i>	<i>0.33</i>	<i>0.09</i>	<i>0.22</i>	<i>0.29</i>	<i>0.03</i>	<i>0.12</i>	<i>0.16</i>
CL1b (n = 15)	65.63	18.12	6.11	2.79	2.02	1.90	0.45	1.34	0.54	0.07	0.21	1.23
	<i>1.65</i>	<i>1.38</i>	<i>0.86</i>	<i>0.27</i>	<i>0.48</i>	<i>0.66</i>	<i>0.15</i>	<i>0.34</i>	<i>0.18</i>	<i>0.06</i>	<i>0.04</i>	<i>0.24</i>
CL1c (n = 2)	65.39	18.91	7.64	2.39	0.93	1.46	0.14	1.16	0.60	0.11	0.27	1.14
	<i>0.07</i>	<i>0.63</i>	<i>0.07</i>	<i>0.23</i>	<i>0.17</i>	<i>0.46</i>	<i>0.00</i>	<i>0.22</i>	<i>0.10</i>	<i>0.01</i>	<i>0.08</i>	<i>0.01</i>
CL1 tot (n = 26)	65.08	17.92	6.07	2.86	2.59	1.86	0.49	1.36	0.58	0.09	0.22	1.26
	<i>1.51</i>	<i>1.21</i>	<i>0.66</i>	<i>0.25</i>	<i>0.84</i>	<i>0.54</i>	<i>0.14</i>	<i>0.29</i>	<i>0.23</i>	<i>0.05</i>	<i>0.08</i>	<i>0.21</i>
Group 1	64.49	19.12	6.22	2.88	2.28	2.02	0.49	1.23	0.41	0.11	n.r.	n.r.
(Foy)	<i>1.36</i>	<i>1.34</i>	<i>0.85</i>	<i>0.26</i>	<i>0.86</i>	<i>0.39</i>	<i>0.12</i>	<i>0.24</i>	<i>0.08</i>	<i>0.04</i>		
Série 2.1	64.42	18.50	7.78	2.54	1.35	1.60	0.16	1.23	0.79	0.18	n.r.	n.r.
(Foy)	<i>1.05</i>	<i>1.22</i>	<i>0.67</i>	<i>0.15</i>	<i>0.65</i>	<i>0.37</i>	<i>0.02</i>	<i>0.15</i>	<i>0.14</i>	<i>0.04</i>		
AQ1a	64.97	17.89	5.70	3.00	3.23	1.78	0.55	1.15	0.54	0.12	0.23	1.22
(Gallo)	<i>1.09</i>	<i>0.81</i>	<i>0.57</i>	<i>0.11</i>	<i>0.57</i>	<i>0.27</i>	<i>0.07</i>	<i>0.15</i>	<i>0.10</i>	<i>0.02</i>	<i>0.05</i>	<i>0.07</i>
AQ1b	65.59	18.66	6.04	2.79	1.76	1.90	0.51	1.04	0.46	0.06	0.26	1.34
(Gallo)	<i>1.64</i>	<i>1.44</i>	<i>0.49</i>	<i>0.26</i>	<i>0.38</i>	<i>0.45</i>	<i>0.11</i>	<i>0.14</i>	<i>0.08</i>	<i>0.02</i>	<i>0.06</i>	<i>0.16</i>
CL2a (n = 3)	69.20	15.91	8.57	2.82	0.40	0.03	0.08	0.63	1.38	0.08	0.14	1.09
	<i>1.17</i>	<i>0.66</i>	<i>1.17</i>	<i>0.03</i>	<i>0.08</i>	<i>0.00</i>	<i>0.01</i>	<i>0.03</i>	<i>0.94</i>	<i>0.06</i>	<i>0.02</i>	<i>0.07</i>
CL2b (n = 3)	67.38	15.49	9.47	2.90	0.53	0.82	0.08	0.61	1.48	0.22	0.14	0.87
	<i>1.27</i>	<i>0.80</i>	<i>1.20</i>	<i>0.04</i>	<i>0.17</i>	<i>0.14</i>	<i>0.03</i>	<i>0.06</i>	<i>0.52</i>	<i>0.08</i>	<i>0.04</i>	<i>0.32</i>
CL2 tot (n = 6)	68.29	15.70	9.02	2.86	0.46	0.43	0.08	0.62	1.43	0.15	0.14	0.98
	<i>1.48</i>	<i>0.70</i>	<i>1.17</i>	<i>0.05</i>	<i>0.14</i>	<i>0.44</i>	<i>0.02</i>	<i>0.05</i>	<i>0.68</i>	<i>0.10</i>	<i>0.03</i>	<i>0.24</i>
Petra	69.81	15.04	9.14	2.86	0.49	0.28	0.09	0.52	0.95	0.15	0.16	0.77
(Schibille)	<i>1.31</i>	<i>0.77</i>	<i>0.72</i>	<i>0.17</i>	<i>0.07</i>	<i>0.29</i>	<i>0.01</i>	<i>0.08</i>	<i>0.29</i>	<i>0.06</i>	<i>0.06</i>	<i>0.09</i>
Jalame (no Mn)	70.43	15.73	8.78	2.72	0.39	0.10	0.09	0.60	0.79	n.r.	n.r.	n.r.
(Brill)	<i>1.20</i>	<i>0.92</i>	<i>0.73</i>	<i>0.14</i>	<i>0.06</i>	<i>0.09</i>	<i>0.01</i>	<i>0.14</i>	<i>0.14</i>			
Jalame (Mn)	69.39	15.95	8.43	2.78	0.55	1.07	0.08	0.59	0.73	n.r.	n.r.	n.r.
(Brill)	<i>1.45</i>	<i>1.01</i>	<i>0.36</i>	<i>0.20</i>	<i>0.34</i>	<i>0.32</i>	<i>0.01</i>	<i>0.10</i>	<i>0.12</i>			
AQ2a	66.85	16.58	9.09	2.92	0.47	1.18	0.08	0.51	1.29	0.16	0.20	0.75
(Gallo)	<i>1.62</i>	<i>0.60</i>	<i>0.94</i>	<i>0.18</i>	<i>0.09</i>	<i>0.22</i>	<i>0.01</i>	<i>0.05</i>	<i>0.28</i>	<i>0.04</i>	<i>0.03</i>	<i>0.19</i>
AQ2b	66.35	17.44	10.03	2.98	0.47	0.14	0.08	0.59	0.82	0.07	0.19	1.38
(Gallo)	<i>1.84</i>	<i>0.95</i>	<i>1.11</i>	<i>0.14</i>	<i>0.15</i>	<i>0.11</i>	<i>0.03</i>	<i>0.06</i>	<i>0.09</i>	<i>0.01</i>	<i>0.07</i>	<i>0.13</i>
CL3 (n = 25)	68.25	18.95	6.70	1.93	0.76	0.66	0.13	0.66	0.57	0.04	0.28	1.30
	<i>1.37</i>	<i>1.10</i>	<i>0.92</i>	<i>0.21</i>	<i>0.39</i>	<i>0.26</i>	<i>0.05</i>	<i>0.17</i>	<i>0.25</i>	<i>0.02</i>	<i>0.08</i>	<i>0.19</i>
Série 3.2	68.07	18.79	6.99	1.92	0.70	0.95	0.09	0.65	0.44	0.08	n.r.	n.r.
(Foy)	<i>1.49</i>	<i>0.85</i>	<i>0.74</i>	<i>0.15</i>	<i>0.15</i>	<i>0.34</i>	<i>0.02</i>	<i>0.16</i>	<i>0.08</i>	<i>0.03</i>		
AQ3	68.40	19.24	6.19	1.95	0.79	0.98	0.12	0.64	0.41	0.05	0.28	1.56
(Gallo)	<i>1.97</i>	<i>1.30</i>	<i>0.52</i>	<i>0.10</i>	<i>0.21</i>	<i>0.25</i>	<i>0.02</i>	<i>0.10</i>	<i>0.04</i>	<i>0.01</i>	<i>0.08</i>	<i>0.18</i>

Mean value and standard deviation (in italics) of the major elements for each of the three groups identified and some reference groups cited in the text are here reported. Reference average compositions are taken from: AQ1, AQ2, AQ3: Gallo et al. [24]; Group 1, Série 2.1, Série 3.2 Foy et al. [25]; Petra: Schibille et al. [26]; Jalame (no Mn), Jalame (with Mn): Brill [27].
n.r. = not reported.

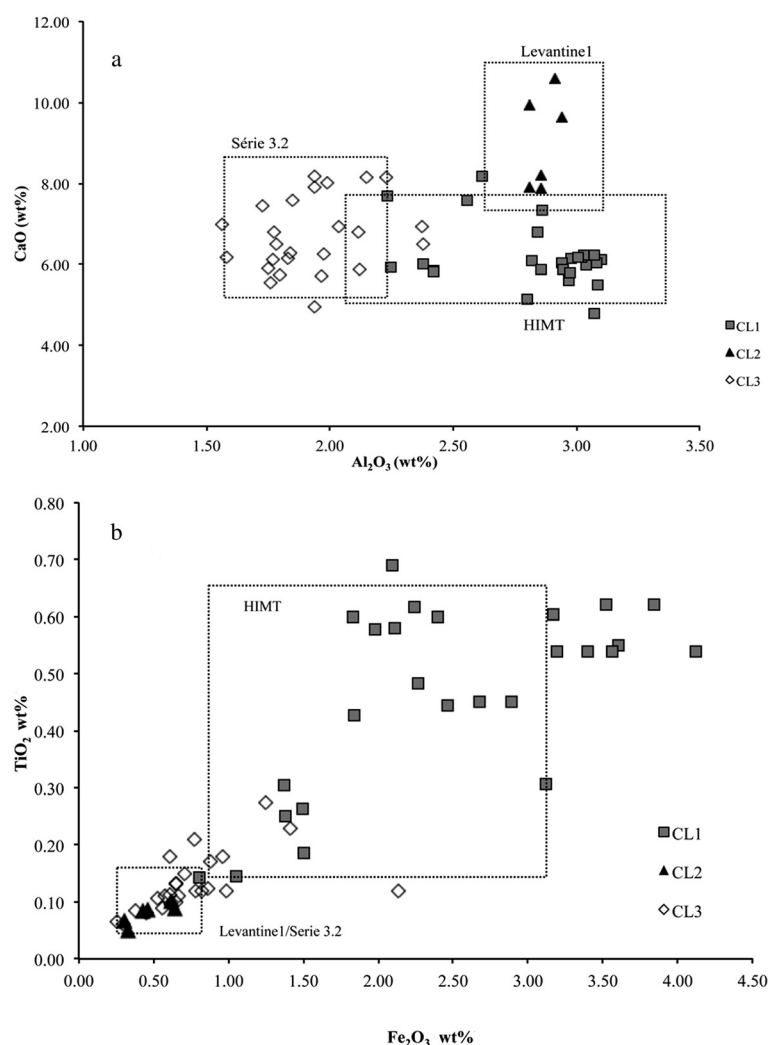


Figure 2 Binary plots. Compositional ranges of reference literature groups are reported in dotted line. **(a)** CaO (wt%) versus Al₂O₃ (wt%). **(b)** TiO₂ (wt%) versus Fe₂O₃ (wt%).

AQ1 [24]). Although primary production sites directly linked with the HIMT composition have not been discovered yet, raw glass characterised by high levels of iron, aluminium, titanium and manganese oxides is thought to have been produced in Egypt between the 4th and the 8th centuries [25,31,32]. However, it should be underlined here that, even though some studies [31] restrict HIMT definition to glass samples that show a positive correlation between iron and alumina, titania and manganese, no correlation has been identified within the HIMT assemblage of Classe. The lack of such diagnostic correlations may be due to the varied mineralogical composition of sands employed in the primary production of HIMT glass at different times and, possibly, in slightly different locations or can also be interpreted as a result of inter-mixing among raw HIMT glass chunks and/or HIMT cullet of different origins.

Together with the uncertainty on its production region, HIMT glass has not been yet well defined compositionally [30]. In particular, the increase in recent years in published data has resulted in the identification of considerable compositional variability within this group, characterised by ever more extreme or low concentrations of some of the characteristic elements, and in its production into “strong” and “weak” HIMT groups, in accordance with terminology used by Foster and Jackson [30]. In this context, HIMT assemblage from Classe, subdivided into the three subgroups (CL1a, CL1b and CL1c which differ mainly for iron content) is quite coherent with the coeval Mediterranean and European HIMT glass.

Samples of group CL1a and CL1b are quite similar to the “strong” HIMT composition such as Group1 by Foy and co-workers [25]. Group 1 starts to be extensively

traded along the Mediterranean shores from the beginning of the 5th century and its circulation seems to stop at the beginning of the 6th and this chronological range is fully consistent with the dating of the site of Classe.

However, the iron content detected in all the samples of group CL1a is indeed very high if compared to those generally reported in the literature for “strong” HIMT glasses [Table 5]. A similar compositional trend was only detected into HIMT glass from Aquileia (North-Eastern Italy) where groups AQ1a and AQ1b [25] well correspond to CL1a and CL1b sub-groups respectively, and this suggests similar commercial routes for these sites, both located along the North Adriatic coast [Table 5].

As far as CL1c group is concerned, we were able to compare it with the “weak” HIMT group, i.e., characterised by lower values of iron, titanium and manganese oxide, such as Série 2.1 of Foy and co-workers [25], dated between the 6th century and the 8th century AD), and/or group HIMT1 of Foster and Jackson [30], dated from the 4th century onwards and identified in British glass assemblages.

Finally among the HIMT glasses of group CL1, sample D26 shows a peculiar composition. The high contents of alumina, titania and iron oxide allow us to assimilate it to the HIMT composition, except for very low manganese [Tables 3 and 4]. Its high iron content may be also due to colouring agents intentionally added, imparting its blue colour. The high titanium content ($\text{TiO}_2=0.43$ wt%) of this sample however is hardly consistent with any other Roman and Late Antique composition, except HIMT. Samples of comparable compositions, characterised by high soda, iron, alumina and titania and very low manganese were already identified by Rehren and Cholacova [33] in Byzantine glasses from Dichin (Bulgaria) and named “HIT” (High Iron and Titanium). Even though it is not possible at the moment to formulate further hypotheses about the specific fragment from Classe, the chronology of the excavations of Classe and Dichin, both dated to the 5th–6th century, allows us to suggest the possibility that sample D26 could be an HIT glass.

Minor and trace elements can provide further useful information to discriminate the quality of sands employed in primary production and to evaluate the level of recycling. Samples included in CL1 have, where measured, high contents of Ba, Zr, V, Cr, Ni, Y [Table 4] deriving from the heavy and mafic minerals naturally contained in the sand of origin, confirming the use of an impure sand. To evaluate the extent of recycling Co, Cu, Pb, Sn, Zn and Sb can be particularly useful; it is generally assumed that low contents of these elements (in the 1–100 ppm range) originated from heavy mineral constituents in the sand [34], whereas their presence in the 100–1000 ppm range may be explained by the recycling of earlier glass and the addition of intentionally coloured glass or cullet during

melting [35]. HIMT samples coming from Classe (groups CL1a and CL1b), show generally low but not negligible levels of the above elements, when detectable, suggesting limited recycling, with the exception of the deeply coloured vessels (the deep green D1 and the blue D26). In sample D1, the high levels of copper and lead oxides can be related to the intentional addition to the batch colouring elements and/or fragments of deeply coloured glass such as mosaic *tesserae* as colouring agents; it is also possible that glass cullet collected for recycling was selected on the basis of the colour and therefore intentionally coloured green glass and/or mosaic *tesserae* could be melted together with green HIMT glasses.

Samples included in group CL2, due to their elevated levels of lime and relatively low iron, titanium and manganese, can be correlated to the glass named Levantine 1 by Freestone and well documented in the literature (Jalame [27], Apollonia and Dor [36]; Group 3 [25]; Petra [26]; Levantine 1a-1b [30], group AQ/2 [24]). Levantine 1 glass was traded along the Mediterranean between the end of the 4th and 7th century AD. Primary production centres for Levantine 1 raw glass were excavated at Jalame [27], Dor [36] and Apollonia-Arsuf, [4] all in the Syro-Palestinian area. A closer observation of group CL2 shows that samples from Classe may be further subdivided into two sub-groups, differing in manganese content: the first named CL2a with negligible Mn (samples D21, G05, T04) and the second named CL2b with $\text{MnO} \geq 0.5$ wt% and thus consistent with an intentional addition of this element (D58, C4, T10). Brill [27] and Foster and Jackson [30] observed the same subdivision into ‘low’ and ‘high’ Mn glass in some samples with Levantine 1 composition from Jalame and Britain, respectively, as Gallo et al. [24] in the *Bestie Ferite* assemblage recognize a similar trend: groups AQ2a and AQ2b from Aquileia, both Levantine 1 in composition, are, in fact, mainly distinguished by the manganese content, that is high in AQ1a and negligible in AQ2b [Table 5].

Group CL3, due to its low content of alumina and lime [Figure 2], and high soda can be related to Série 3.2 composition, first identified by Foy and co-authors [27] among glass found in France, Tunisia, Lybia, Lebanon and Egypt. This composition is dated between the end of the 5th century and the beginning of the 6th century AD and even if sand deposits and primary working sites have not been identified yet, they are thought to be in the Levantine coast. The interpretation of trace elements confirms the use in group CL3 of a pure sand low in mafic and heavy minerals: comparing the trace elements of group CL3 and group CL1, the former show clearly lower values for V, Cr, Ni, Y, Zr and Ba than the latter [Table 4]. Furthermore group CL3 presents, as expected, very low levels of Co, Cu, Pb, Sb and Zn, and any sign of recycling can be deduced from the samples under

investigation, with the exception of D7, deeply coloured in blue, in which the very high content of lead, copper and cobalt is related to the intentional addition of colouring elements and/or coloured cullet.

Glass similar to Série 3.2 was also identified in Aquileia [24], although in smaller amount than in Classe.

In this context, it should be underlined here that, although the compositional groups identified are the same in Classe and Aquileia, the relative proportions are quite different between two sites. In Classe most of the samples are made of glass HIMT (43%) and Série 3.2 (45%) while the Levantine 1 (12%) composition was found only in a few samples and no raw glass chunks. In Aquileia, the HIMT group dominates the assemblage (61%), followed by glass similar to Levantine 1 (24%) and Série 3.2 (15%) and no raw glass was found in any groups. These differences in proportions between Classe and Aquileia may be only speculated at the moment, relating these to the not perfect coincidence of “life-times” of the two sites (4th-6th centuries AD for “*Casa delle Bestie Ferite*” in Aquileia and 5th-8th centuries for Classe) and/or the periods of maximum diffusion of compositional groups identified, but further studies are surely required to clarify this evidence. On the contrary, the lack of glassworking wastes in Aquileia may easily relate to the different functions of the excavated areas, a productive complex in the case of Classe and a *domus* in the case of Aquileia.

Comparing the most represented archaeological forms and compositional groups here identified, some correlations between type and chemical composition were highlighted: among the analysed samples all the Isings 96 beakers, common drinking vessels, belong to group CL1 and can be assimilated to HIMT composition; goblets Isings 111, common but more elaborated drinking vessel, are instead included in group CL3 and appear to be similar to the Série 3.2. Conversely, beakers Isings 106 seem to be produced in all the three compositional groups. It may be hypothesised that Levantine 1 glass was not available for workshops dedicated to the shaping of Isings 96 and Ising 111 in Classe. In addition, comparisons among the common types found in Aquileia and Classe (i.e., beaker Is. 106 and goblet Is. 111) allow us to identify analogies and differences between the two sites. Beakers Ising 106 are made in glass belonging to all the three compositional groups identified in both sites (i.e., HIMT, Levantine 1 and Série 3.2), although they show different relative distributions: beakers Isings 106 from Classe present all the three compositions almost equally represented, while in Aquileia the largest part of the beakers Isings 106 are made with HIMT glass, a smaller part is made with Levantine 1 composition and only a sporadic sample is made with Série 3.2 glass [24]. Goblets Isings 111 from Classe are made with

Série 3.2 glass only, while in Aquileia they are made with Série 3.2, HIMT and Levantine 1 glass in almost equal proportions.

Isotopic analysis

Recent studies have demonstrated the great potential of isotopic analysis for glass provenance study in the case of Roman, Late Antique and Byzantine glass [22,37-40].

Due to the negligible effect of thermic treatments on the isotopic ratios, these analyses represent a useful tool to link a glass object to the source of raw materials employed in primary production. In particular, Sr and Nd isotopic ratios can help locating the source of sand supply used for glass production. Sr is, in fact, expected to be introduced in the glass mainly from the carbonatic fraction of the sand. Sea shells are made of aragonite, while continental limestone is mainly constituted of calcite. Aragonite can bear a considerable amount of the larger ion Sr²⁺ in substitution with Ca²⁺ (9-coordinated) and it is therefore considered the main source of Sr in Roman and Byzantine glass. On the other hand, significant amounts of Sr can also be introduced by Sr-bearing, non-carbonate minerals that are naturally present in sand deposits such as feldspars and other silicatic phases in which Sr²⁺ replaces K⁺. Brems recently noted that, at least for the Western Mediterranean sediments, the Sr isotopic ratio of the sand (generally indicated as ⁸⁷Sr/⁸⁶Sr) can be indicative of the carbonatic fraction only in the case of sediments low in feldspars, with an Al₂O₃/CaO ratio lower than 0.25 [35]. In sands with a higher value the isotopic ratio is due to both sea shells and non-quartz silicatic minerals.

The isotopic ratio of Holocene beach sands, in which the carbonatic fraction is predominantly made of mollusc shells, is expected to be similar to the one of the modern sea-water (≈0.7092); the one of sediments rich in aged limestone is expected to be around 0.7080 [41].

Therefore Roman, Late Antique and Byzantine glass, produced with coastal sand rich in sea shells, is expected to have a Sr isotopic ratio similar to 0.7092.

Nd is another useful provenance marker for ancient glass. In Roman, Hellenistic and Byzantine glass, Nd is introduced by the heavy, non-quartz, silicatic fraction of the sand [39] and being a rare earth element (REE), contamination from other sources and recycling can be excluded [41].

Along the Mediterranean coast, the isotopic ratio for Nd (usually expressed as εNd) of coastal sands show an East to West gradient from the slightly negative value of the Nile delta (εNd = -1) to the strongly negative values of southern Spain (-12) and Western Sahara (-13) [39]. Sands from the Syro-Palestinian and Egyptian coast, where primary production sites were discovered and that are supposed to be the sources of sand for Roman, Late

Antique and Byzantine glass, have an ϵNd between -5 and -6 . The same values are therefore expected for primary glasses coming from this area, such as HIMT and Levantine 1.

To trace the provenance of the raw materials employed for the primary production of the glass excavated in Classe, analysis of the isotopic ratios for Sr and Nd was performed on 12 samples selected on the basis of the following criteria: 1) suitable dimension of the fragment; 2) availability of trace element data; 3) low levels of recycling indicators. The complete results of isotopic analyses are given in [Table 6].

All the analysed glasses have a Sr content ranging between 366 and 584 ppm [Table 4] that is consistent with the hypothesis of the use of coastal sand rich in mollusc shells [35].

The $^{87}\text{Sr}/^{86}\text{Sr}$ ratio varies among the samples from a maximum value of 0.70916 to a minimum of 0.70829. As shown in the biplot diagram in which the isotopic ratio is plotted *versus* the Sr content [Figure 3a], samples can all be allocated between the value of modern sea-water (and Holocene coastal sand deposits), i.e., 0.7092, and the one of aged limestone, i.e., 0.7080. In more detail, the lower isotopic ratio found in samples of CL1 group (characterised by HIMT composition) shows a lower isotopic ratio, more similar to the characteristic value for continental limestone if compared to groups CL3 (Série 3.2) and CL2 (Levantine 1) [Figure 3a]. The use of limestone-rich sand for the primary production of these two groups can be excluded, as the high content of Sr is, without any doubt, consistent with the use of aragonitic marine shells as a source of CaO. The smaller isotopic ratio found in CL1 samples can therefore be indicative of the use, in this specific group, of an impure coastal sand rich in non-carbonatic, Sr-bearing silicatic minerals.

The different origin of Sr in the samples under examination can be confirmed by a binary diagram where

Table 6 Isotopic composition of the selected samples

Sample	Group	$^{87}\text{Sr}/^{86}\text{Sr}$	2σ	$^{143}\text{Nd}/^{144}\text{Nd}$	2σ	ϵNd
D24	CL1	0.70841	0.00007	0.512425	0.000053	-4.15
D5	CL1	0.70849	0.00007	0.512380	0.000064	-5.02
FD	CL1	0.70829	0.00007	0.512409	0.000053	-4.48
PVS	CL1	0.70840	0.00005	0.512362	0.000048	-5.38
TB	CL1	0.70845	0.00007	0.512382	0.000057	-4.99
C4	CL2	0.70903	0.00006	0.512438	0.000058	-3.91
A3	CL3	0.70897	0.00007	0.512393	0.000058	-4.79
D16	CL3	0.70916	0.00007	0.512396	0.000054	-4.73
D23	CL3	0.70884	0.00007	0.512387	0.000051	-4.90
D25	CL3	0.70892	0.00006	0.512401	0.000053	-4.62
PV	CL3	0.70871	0.00007	0.512404	0.000054	-4.57
PVA	CL3	0.70909	0.00006	0.512373	0.000053	-5.17

Measured values of the isotopic ratio for Sr and Nd, ϵNd and internal precision 2σ are here reported.

$^{87}\text{Sr}/^{86}\text{Sr}$ is plotted versus CaO (wt%) [Figure 3b]: samples of group CL1 and CL3 have comparable calcium contents but different isotopic ratios; given that the calcium source is seashells for all the analysed samples, this evidence suggests that the Sr isotopic ratio in group CL1 may be not entirely due to the carbonates, and it may also be influenced by other minerals.

Isotopic data for ϵNd range between -5.38 and -3.91 in all the analysed fragments. These values are clearly consistent with an Eastern Mediterranean origin of the sand but they are, on average, less negative than expected for Middle-Eastern glasses such as Levantine 1 and HIMT [42], expected to fall between -6 and -5 [Figure 3c]; this evidence can therefore indicate the use, for the glass primary production of all the three compositions, of a slightly different sand deposits, more influenced by the Nile sediments, geologically “young” and

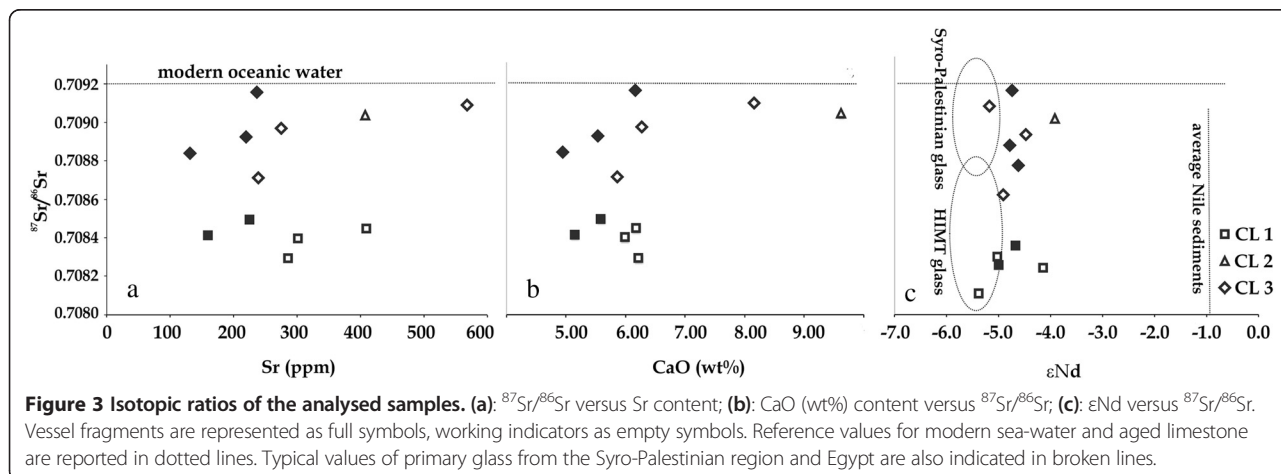


Figure 3 Isotopic ratios of the analysed samples. (a): $^{87}\text{Sr}/^{86}\text{Sr}$ versus Sr content; **(b):** CaO (wt%) content versus $^{87}\text{Sr}/^{86}\text{Sr}$; **(c):** ϵNd versus $^{87}\text{Sr}/^{86}\text{Sr}$. Vessel fragments are represented as full symbols, working indicators as empty symbols. Reference values for modern sea-water and aged limestone are reported in dotted lines. Typical values of primary glass from the Syro-Palestinian region and Egypt are also indicated in broken lines.

therefore less negative, that can be interpreted a slightly different shore segment, probably located in Egypt. The scarcity of isotopic data on Late Antique glasses does not allow us to formulate more detailed conclusions and further studies are required.

Conclusions

The present study was conducted with the aim of throwing new light upon the production, trade and consumption of glass in the area of Classe during the Late Antiquity.

In the 5th century a secondary glass workshop was active in the area of the harbour. The archaeological study revealed that this workshop was dedicated to the shaping of glass vessels starting from raw glass chunks and, possibly, cullet. Evidence of glass re-melting (raw chunks, lumps, etc.) and glass-blowing (moils, pontil scars etc.) were in fact identified, but no evidence of glass primary production was found. Samples selected among glassworking wastes and the most represented and common type of drinking vessels from the two contexts of Building 6 and dump US4381 were here archaeometrically analysed.

In accordance with the dating of the site, all the analysed fragments are silica-soda-lime glasses, produced with natron as a flux, and belong to the Late-Antique compositional groups HIMT, Série 3.2 and Levantine 1.

The differences in the chemical composition of the three groups here identified reflect the different sand sources employed: impure and rich in heavy minerals for CL1 (HIMT), pure and rich in carbonates for CL2 (Levantine 1), pure and low in Al-bearing minerals and carbonates for group CL3 (Série 3.2). Isotopic analysis also confirmed that different sources of sands were used in samples of groups CL2-3 and CL1: all three groups derive from Holocene coastal sands rich in mollusc shells and isotopically located in the eastern-Mediterranean shore but, if CL2 and CL3 seem to have been produced from Syro-Palestinian deposits, CL1 appears to derive from a more impure sand, influenced by the Nile contribution and probably located in Egypt. Furthermore, a slight shift in the isotopic signature with respect to the published data is remarked, suggesting that Classe was supplied by different Eastern Mediterranean locations.

The Eastern Mediterranean isotopic signature found in all the samples from Classe is in accordance with a centralized primary production model. It is reasonable that Classe, as harbour of the capital city of the Empire, strongly linked to the Levantine region, imported raw chunks from Eastern Mediterranean primary production centres to supply local secondary workshops. It is also reasonable that cullet was occasionally collected and re-melted together with fresh raw glass, although the analysed samples do not show strong evidence of recycling.

The presence among the finds of raw glass chunks, glassworking wastes and vessels of similar composition can be interpreted as evidence of a systematic glassworking activity although limited to HIMT and Série 3.2 glass. The lack of chunks and the scarcity of finds of the compositional group Levantine 1, in fact, does not allow any consideration about systematic trade or working activities for glass of this composition.

Systematic comparisons between Classe and Aquileia, the two most important Late-Antique archaeological sites of North-Eastern Italy, were also carried out in order to clarify better the role of the Northern Adriatic area in the glass production, trade and consumption during the Late-Roman/Early Medieval period. Comparisons show that during the Late Antiquity Classe and Aquileia seem to be supplied of raw glass by the same trade routes: HIMT, Levantine 1 and Série 3.2 compositions were identified, although Série 3.2 in the *Bestie Ferite* (Aquileia) assemblage is less well represented if compared with Classe. In addition, some interesting correlations between types and chemical composition were here highlighted. However, in order to clarify the real range of this evidence, and eventually to establish systematic links between supply routes, technological choices and specific locations, further systematic studies, carried out with similar methodological approach, are required.

Abbreviation

OM: Optical microscopy; SEM: Scanning electron microscopy; EPMA: Electron probe micro analysis; XRF: X-ray fluorescence; XRPD: X-ray powder diffraction; MC-ICP-MS: Multi collector- inductively coupled plasma- mass spectrometry; REE: Rare earth elements.

Competing interests

The authors declare that they have no competing interests.

Authors' contributions

TC and EC made the archaeological study; SM performed chemical and isotopic analyses; SM, AS, MV, GM contributed to the interpretation of analytical data. All authors read and approved the final manuscript.

Acknowledgements

The authors would like to thank the "Soprintendenza per i Beni Archeologici dell'Emilia Romagna" for authorizing the present study and prof. A. Augenti (Università degli Studi di Bologna) for providing the glass samples. They are also grateful to prof. P. Degryse and co-workers (Katholieke Universiteit Leuven and Ghent University) for their kind support during the isotopic analyses; dr. D. Pasqual for the XRF analyses; R. Carampin (C.N.R. Istituto di Geoscienze e Georisorse, Sezione di Padova) for the EPMA analyses.

This work was carried out with the financial support of PRIN 2009 "Continuità e discontinuità nelle produzioni vetrarie altoadriatiche" tra il IX sec. a.C. e il XIV sec. d.C. (prot. 2009MC8FA8).

Author details

¹Dipartimento di Beni Culturali, Università degli Studi di Padova, piazza Capitanato 3, Padova, Italy. ²Dipartimento di Storia Culture Civiltà, Alma Mater Studiorum Università degli Studi di Bologna, piazza San Giovanni in Monte 2, Bologna, Italy. ³Dipartimento di Beni Culturali, Alma Mater Studiorum Università degli Studi di Bologna - Sede di Ravenna, via degli Ariani 1, Ravenna, Italy. ⁴Dipartimento di Geoscienze, Università degli studi di Padova, Via Giovanni Gradeno 6, Padova, Italy.

Received: 20 June 2014 Accepted: 26 January 2015

Published online: 25 March 2015

References

- Tontini S. Vetri e produzione vetraria a Classe (Ravenna) in età tardoantica e altomedievale. *Bulletin. Association pour L'Antiquité Tardive*. 2006;15:45–55.
- Cirelli E, Tontini S. Produzione vetraria a Classe nella tarda antichità. In: Vandini M, editor. *Riflessioni e trasparenze: diagnosi e conservazione di opere e manufatti vetrosi*, Proceeding of the A.I.Ar. Conference, Ravenna 24th -26th February 2009. Bologna: Patron Ed; 2010. p. 125–33.
- Nenna MD, Vichy M, Picon M. L'atelier de verrier de Lyon, du I^{er} siècle après J.-C., et l'origine des verres 'romains'. *Revue d'Archéométrie*. 1997;21:81–7.
- Gorin-Rosen Y. The ancient glass industry in Israel. Summary of the finds and new discoveries. In: Nenna MD, editor. *La Route du Verre: Ateliers primaires et secondaires du second millénaire av. J.-C. au Moyen-Age*. Lyon: Maison de l'Orient Méditerranéen; 2000. p. 49–64.
- Freestone IC, Ponting M, Hughes MJ. The origins of Byzantine glass from Maroni Petrea. *Cyprus Archaeometry*. 2002;44(2):257–72.
- Augenti A, Cirelli E. From suburb to port: the rise (and fall) of Classe as a centre of trade and redistribution. In: Keay S, editor. *Rome, Portus and the Mediterranean*, vol. 21. Rome: Archaeology Monographs of the British School at Rome; 2012. p. 205–21.
- Cirelli E. Typology and diffusion of Amphorae in Ravenna and Classe between the 5th and the 8th centuries AD. In: Poulou-Papadimitriou N, Nodarou E, Kilikoglou V, editors. *Late Roman Coarse Wares, Cooking Wares and Amphorae in the Mediterranean*. Archaeology and archaeometry. Proceedings of the 4th International Conference (Thessaloniki, 7–10 April 2011). Oxford: Archaeopress Publishers of British Archaeological Reports; 2014. p. 541–52.
- Cirelli E, Cannavici A. A 6th century dump from Classe (Ravenna). In: Poulou-Papadimitriou N, Nodarou E, Kilikoglou V, editor. *Late Roman Coarse Wares, Cooking Wares and Amphorae in the Mediterranean*. Archaeology and archaeometry. Proceedings of the 4th International Conference (Thessaloniki, 7–10 April 2011). Oxford: Archaeopress Publishers of British Archaeological Reports; 2014. p. 963–74.
- Bierbrauer V. Stengelgläser. In: Bierbrauer V, editor. *In villino-Ibligo in Friaul 1: die römische Siedlung und das späntantik-frühmittelalterliche Castrum*. München: C.H. Beck'sche Verlagbuchhandlung; 271–287.
- Foy D. Le verre de la fin du I^{er} au VIII^e siècle. In: Foy D, editor. *Le verre de l'Antiquité tardive et du haut Moyen Age: typologie, chronologie, diffusion*. Association française pour l'archéologie du verre (huitième rencontre, Guiry-en-Vexin 18–19 novembre 1993). Guiry-en-Vexin: Musée archéologique départemental du Val d'Oise; 1995. p. 187–242.
- Jennings S. The Roman and Early Byzantine glass from the Souks excavations: an interim statement. *Berytus*. 1998;43:111–46.
- Sagui L. Produzioni vetrarie a Roma tra V e VII secolo. In: *Annales du 14^e Congrès de l'Association Internationale pour l'Histoire du Verre (Venezia-Milano, 1998)*. Lochem: AIHV; 2000. p. 203–7.
- Falcetti C. La suppellettile in vetro. In: Mannoni T, Murialdo G, editors. S. Antonino: un insediamento fortificato nella Liguria bizantina. Bordighera: Istituto internazionale di studi liguri; 2001. p. 403–54.
- Jennings S, Abdallah J. Roman and later blown glass from the Aub excavations in Beirut (Sites Bey 006, 007 and 045). *ARAM*. 2002;13–14:237–64.
- Foy D. In: Ben Abed-Ben Khader A, editor. *Sidi Jdidi I - La Basilique Sud*. Rome: École française de Rome; 2004. p. 317–29.
- Isings C. Roman glass from dated finds. Groningen, Djakarta: Wolters; 1957.
- Sternini M. Il vetro in Italia tra V e IX secolo. In: Foy D, editor. *Le verre de l'Antiquité tardive et du haut Moyen Age : typologie, chronologie, diffusion*. Association française pour l'archéologie du verre (huitième rencontre, Guiry-en-Vexin 18–19 novembre 1993). Guiry-en-Vexin: Musée archéologique départemental du Val d'Oise; 1995. p. 243–89.
- Fiori C, Vandini M. Produzione di vetro a Classe (Ravenna) nel V-VI sec d.C. *Rivista della Stazione Sperimentale del Vetro*. 2010;5:15–24.
- Fiori C. Mosaic tesserae from the Basilica of San Severo and glass production in Classe, Ravenna, Italy. In: James L, Entwistle C, editors. *New light on old glass: recent research on Byzantine mosaics and glass*. The British Museum; 2014:33–41.
- Silvestri A, Marcante A. The glass of Nogara (Verona): a "window" on production technology of mid-Medieval times in Northern Italy. *J Archaeol Sci*. 2011;38(10):2509–22.
- Silvestri A, Molin G, Pomero V. The stained glass window of the southern transept of St. Anthony's Basilica (Padova, Italy): study of glasses and grisaille paint layers. *Spectrochim Acta Part B At Spectrosc*. 2011;66(1):81–7.
- Ganio M, Latruwe K, Brems D, Muchez P, Vanhaecke F, Degryse P. The Sr-Nd isolation procedure for subsequent isotopic analysis using multi-collector ICP-mass spectrometry in the context of provenance studies on archaeological glass. *J Anal At Spectrom*. 2012;27(8):1335–41.
- Shortland J, Degryse P, Walton M, Geer M, Lauwers V, Salou L. The evaporitic deposits of Lake Fazda (Wadi Natrun, Egypt) and their use in roman glass production. *Archaeometry*. 2011;53(5):916–29.
- Gallo F, Marcante A, Silvestri A, Molin G. The glass of the "Casa delle Bestie Ferite": a first systematic archaeometric study on Late Roman vessels from Aquileia. *J Archaeol Sci*. 2014;41:7–20.
- Foy D, Nenna MD. Caractérisation des verres de la fin de l'Antiquité en Méditerranée occidentale: l'émergence de nouveaux courants commerciaux. *Actes Du Colloque De l'Association Française Pour l'Archéologie Du Verre: 7-9th June 2001; Aix-en-Provence*. Marseille, Montagnac: Monique Mergoil; 2003.
- Schibille N, Marii F, Rehren T. Characterization and provenance of late antique window glass from the Petra Church in Jordan. *Archaeometry*. 2008;50(4):627–42.
- Brill RH. Scientific investigations of the Jalame glass and related finds. In: Davidson Weinberg G, editor. *Excavations at Jalame: site of a glass factory in late roman Palestine*. Columbia (MO): University of Missouri Press; 1988. p. 257–94.
- Freestone IC. Chemical analysis of raw glass fragments., N4. In: Hurst HR, editor. *Excavation at Carthage, The Circular Harbour, North Side. The Site and Finds Other than Pottery*, vol. 2. Oxford: Oxford University Press; 1994. p. 290.
- Mirti P, Casoli A, Appolonia L. Scientific analysis of Roman glass from Augusta Praetoria. *Archaeometry*. 1993;35:225–40.
- Foster HE, Jackson CM. The composition of 'naturally coloured' late Roman vessel glass from Britain and the implications for models of glass production and supply. *J Archaeol Sci*. 2009;36(2):189–204.
- Freestone IC, Wolf S, Thirlwall M. The production of HIMT glass: elemental and isotopic evidence. 16th ed. London: *Annales Du 16^e Congrès De l'Association Internationale Pour l'histoire Du Verre*; 2005. p. 153–7.
- Leslie KA, Freestone IC, Lowry D, Thirlwall M. The provenance and technology of near eastern glass: oxygen isotopes by laser fluorination as a complement to Strontium. *Archaeometry*. 2006;48(2):253–70.
- Rehren T, Cholacova A. The early Byzantine HIMT glass from Dichin, Northern Bulgaria. *Interdisciplinary Stud*. 2010; 22–3.
- Wedepohl KH, Baumann A. The use of marine mollusk shells for Roman glass and local raw glass production in the Eifel area (western Germany). *Naturwissenschaften*. 2000;87(3):129–32.
- Jackson CM. From Roman to early Medieval glasses. Many happy returns or a new birth? *Annales Du 13^e Congrès De l'Association Internationale Pour l'histoire Du Verre*: Loche; 1996, 289–301.
- Freestone IC, Gorin-Rosen Y, Hughes MJ. Primary Glass from Israel and the Production of Glass in Late Antiquity and the Early Islamic Period. In: Nenna MD, editor. *La Route du Verre. Ateliers Primaires et Secondaires du Second Millénaire av. JC au Moyen Age*. Lyon: Maison de L'orient Mediterranéen; 2000. p. 65–83.
- Freestone IC, Leslie KA, Thirlwall M, Gorin-Rosen Y. Strontium isotopes in the investigation of early glass production: byzantine and early Islamic Glass from the Near East. *Archaeometry*. 2003;45(1):19–32.
- Brems D, Ganio M, Latruwe K, Balcaen L, Carremans M, Gimeno D, et al. Isotopes on the beach, part 1: strontium isotope ratios as a provenance indicator for lime raw materials used in Roman glass-making. *Archaeometry*. 2013;55:214–34.
- Brems D, Ganio M, Latruwe K, Balcaen L, Carremans M, Gimeno D, et al. Isotopes on the beach, part 2: Neodymium isotopic analysis for the provenancing of roman glass-making. *Archaeometry*. 2013;55:449–64.
- Degryse P, Schneider J. Pliny the Elder and Sr-Nd isotopes: tracing the provenance of raw materials for Roman glass production. *J Archaeol Sci*. 2008;35(7):1993–2000.

41. Degryse P, Henderson J, Hodgins G. Isotopes in vitreous materials: a state-of-the-art and perspectives. In: Degryse P, Henderson J, Hodgins G, editors. *Isotopes in vitreous materials*. Leuven: Leuven University Press; 2009. p. 15–30.
42. Freestone IC, Wolf S, Thirlwall M. Isotopic composition of glass from the Levant and the south-eastern Mediterranean region. In: Degryse P, Henderson J, Hodgins G, editors. *Isotopes in vitreous materials*. Leuven: Leuven University Press; 2009. p. 31–52.

Publish with **ChemistryCentral** and every scientist can read your work free of charge

“Open access provides opportunities to our colleagues in other parts of the globe, by allowing anyone to view the content free of charge.”

W. Jeffery Hurst, The Hershey Company.

- available free of charge to the entire scientific community
- peer reviewed and published immediately upon acceptance
- cited in PubMed and archived on PubMed Central
- yours — you keep the copyright

Submit your manuscript here:
<http://www.chemistrycentral.com/manuscript/>



ChemistryCentral